European Radiology (2018) 28:4379–4388
https://doi.org/10.1007/s00330-018-5407-1

COMPUTED TOMOGRAPHY

Assessment of an advanced virtual monoenergetic reconstruction technique in cerebral and cervical angiography with third-generation dual-source CT: Feasibility of using low-concentration contrast medium

Lu Zhao[1] · Fengtan Li[1] · Zewei Zhang[1] · Zhang Zhang[1] · Yingjian Jiang[1] · Xinyu Wang[1] · Jun Gu[2] · Dong Li[1]

Received: 26 June 2017 / Revised: 13 February 2018 / Accepted: 22 February 2018 / Published online: 13 April 2018

Abstract

Objectives To investigate the feasibility of low-concentration contrast media (LC-CM) in cerebral and cervical dual-energy CT angiography (DE-CTA) using an advanced monoenergetic (Mono+) reconstruction technique.

Methods Sixty-five consecutive patients prospectively selected to undergo cerebral and cervical DE-CTA were randomised into two groups: 32 patients (63.7 ± 9.7 years) in the high-concentration contrast medium (HC-CM) group with iopromide 370 and 33 patients (60.7 ± 10.8 years) in the low-concentration contrast medium (LC-CM) group with iodixanol 270. Traditional monoenergetic (Mono) and Mono+ images from 40 to 100 keV levels (at 10-keV intervals) and the standard mixed (Mixed, 120 kVp equivalent) images were reconstructed. Subjective image quality parameters included the contrast-to-noise ratio (CNR) and objective image quality parameters were evaluated and compared between the two groups.

Results The 40-keV Mono+ images in the LC-CM group showed comparable objective CNR (common carotid arteries: 83.7 ± 24.5 vs. 78.1 ± 23.2; internal carotid arteries: 82.2 ± 26.8 vs. 76.8 ± 24.1; middle cerebral arteries: 72.5 ± 24.6 vs. 70.6 ± 19.2; all $p > 0.05$) and subjective image scores (3.95 ± 0.19 vs. 3.83 ± 0.35; $p > 0.05$) compared with Mixed images in the HC-CM group.

Conclusion The Mono+ reconstruction technique could reduce the concentration of iodinated CM in the diagnosis of cerebral and cervical angiography.

Key Points

- *Mono+ shows decreased noise and superior CNR compared with Mono.*
- *The 40-keV Mono+ images show the highest CNR in the LC-CM group.*
- *The Mono+ reconstruction technique could reduce the concentration of iodinated CM.*

Keywords Cerebral arteries · Carotid arteries · Computed tomography angiography · Monoenergetic imaging · Low-concentration contrast medium

Abbreviations

AA	Ascending aorta
CCA	Common carotid arteries
CIN	Contrast-induced nephropathy
CM	Contrast medium
CNR	Contrast-to-noise ratio
CTA	Computed tomographic angiography
DE-CT	Dual-energy CT
DS-CT	Dual-source CT
HC-CM	High-concentration contrast medium
HU	Hounsfield units
ICA	Internal carotid arteries
LC-CM	Low-concentration contrast medium
MCA	Middle cerebral arteries
Mixed	Standard mixed
Mono	Traditional monoenergetic
Mono+	Advanced monoenergetic
ROI	Region of interest
SD	Standard deviation

Electronic supplementary material The online version of this article (https://doi.org/10.1007/s00330-018-5407-1) contains supplementary material, which is available to authorized users.

✉ Dong Li
dr_lidong@163.com

[1] Department of Radiology, Tianjin Medical University General Hospital, Tianjin 300052, China

[2] Siemens Healthineers, Beijing 100102, China

Introduction

Computed tomographic angiography (CTA) examination has been increasingly used to assess cerebral and cervical vessels clinically. Potential nephrotoxicity is one of the major concerns associated with CTA, which requires administration of iodinated contrast medium (CM) [1, 2]. In fact, contrast-induced nephropathy (CIN) could be as high as the third most common cause of acute kidney injury in patients admitted to hospital, after ischaemic and drug-induced injury [3]. It is more likely for CIN to occur in patients with risk factors including pre-existing renal impairment, diabetes mellitus, congestive heart failure, and old age [4]. The dose of CM, which is linearly proportional to the CM concentration, is an important risk factor, and the higher the dose is, the higher the risk and severity of CIN [1, 5]. Some studies have indicated that a high CM concentration showed a predominant toxic effect on renal tubules [6, 7]. It is therefore desirable to have a low-concentration contrast medium (LC-CM) in CTA. In CTA, the magnitude of arterial enhancement increases in direct proportion to the rate of iodine delivery, which is proportional to the product of the injection rate and CM concentration [8]. LC-CM results in decreased vascular attenuation under the same injection volume and flow rate compared with HC-CM [9]. Low kilovoltage (kVp) levels have been shown to improve contrast enhancement in CTA, which could compensate for decreased vascular attenuation caused by LC-CM [10, 11]. However, the disadvantage of this method lies in the increased image noise, which can potentially affect the image quality and the subsequent accuracy of diagnosis.

Monoenergetic images generated in image space from dual-energy CT (DE-CT) data can be derived using a post-processing technique, which allows for calculation of images at any desired hypothetical energy level from 40 to 190 keV. It has the potential to optimise contrast and noise [12]. The traditional monoenergetic (Mono) reconstruction technique has shown its capability to improve image quality at low keV levels because of the increased iodine enhancement in cerebral and cervical CTA [13], pulmonary CTA [14], coronary CTA [15] and lower extremity CTA [16]. The optimum contrast-to-noise ratio (CNR) in Mono images was found to be between 60 and 80 keV, and CNR decreased with the increased noise level at energy levels lower than 60 keV. Therefore, energy levels lower than 60 keV were not recommended for clinical application with the Mono technique. Recently, a noise-optimised advanced monoenergetic (Mono+) reconstruction technique has been developed to improve image quality in contrast-enhanced DE-CT particularly at ultra-low keV levels [17]. The Mono+ technique uses a regional spatial frequency-based recombination of the high signal at lower energies and the superior noise properties at medium energies. Thus Mono+ images have better CNR than Mono at energy levels lower than 60 keV [18–23]. This would potentially allow for a reduced concentration of CM because of the optimised CNR at lower keV levels.

To the best of our knowledge, no previous report has studied cerebral and cervical angiography obtained by using LC-CM and the Mono+ technique. Therefore, the purpose of the present study was to prospectively investigate the potential for reducing the CM concentration by using the Mono+ technique in cerebral and cervical DE-CTA.

Materials and methods

Patient population

This prospective study was approved by the institutional ethics review board of Tianjin Medical University General Hospital. Written informed consents were obtained from all patients. Sixty-five consecutive patients with clinical suspicion of vessel occlusion or dissection scheduled to undergo cerebral and cervical CTA were prospectively selected. Exclusion criteria included contraindication to intravenous administration of iodine CM and the presence of renal dysfunction or renal failure. The 65 patients were randomised into two groups: 32 patients in the HC-CM group received iopromide 370 as CM (370 mg I/ml, Bayer Schering Pharma) and 33 patients in the LC-CM group received iodixanol 270 as CM (270 mg I/ml, GE Healthcare).

Image acquisitions

All data sets were acquired on a 192-slice dual-source CT (DS-CT) system (SOMATOM Force, Siemens Healthineers, Germany). The scan was performed in caudocranial direction from the ascending aorta to the apex of the skull. Bolus tracking was automatically triggered at 100 Hounsfield units (HU) in the descending thoracic aorta. Settings were as follows: pitch 0.7; collimation 2 * 64 * 0.6 mm; rotation time 0.25 s; 80 kV/120 ref. mAs for tube A, Sn150 kV (with tin filter)/80 ref. mAs for tube B. Automatic exposure control (CAREdose 4D) was used. CM was injected at a dose of 0.5 ml/kg body weight on the patient's forearm with a flow of 3.5 ml/s followed by 40 ml saline solution.

Image reconstruction

DE-CT raw data were reconstructed using a soft tissue convolution kernel with dedicated advanced modelled iterative reconstruction (ADMIRE, Hr36, Siemens Healthineers). All data sets were post-processed on a dedicated dual-energy 3D multi-modality workstation (syngo.via, version VA30A, Siemens Healthineers). All series were reconstructed as axial images with a section thickness of 1.0 mm. The standard mixed (Mixed) images at a weighting factor of 0.8 combining

80% of the low kV with 20% of the high kV spectrum were reconstructed, representing a single-energy acquisition at 120 kVp [24]. Mono and Mono+ images were reconstructed at the same energy levels with 10-keV intervals ranging from 40 to 100 keV. Fifteen different reconstructions were evaluated in each patient, including (1) Mixed, (2) Mono at the 40, 50, 60, 70, 80, 90 and 100-keV levels and (3) Mono+ at 40, 50, 60, 70, 80, 90 and 100-keV levels.

Image assessment

Objective image analysis

One radiologist with 3 years of experience in interpreting cerebral and cervical CTA performed objective measurements. Attenuations were measured in the ROIs: ascending aorta (AA) at the level of the aortic pulmonic window, bifurcation of the common carotid arteries (CCA), siphon of the internal carotid arteries (ICA) and proximal segment of the middle cerebral arteries (MCA). On the four levels above, additional ROIs were placed at the pectoralis major muscle, sternocleidomastoid muscle and cerebral tissues, respectively. All vessel ROIs were made as large as possible according to sizes performed in the central parts of the vessel without pathological findings. In the presence of significant luminal narrowing, vessel attenuation was measured distal to the stenosis. Completely occluded or aplastic segments were not evaluated. All muscle ROIs were made as large as possible according to sizes. Attenuations of the cerebral tissues consisting of both white and grey matter were measured near the measured vessels, avoiding vascular structures, using a 2.0 cm^2 ROI. The mean CT attenuations for individual subjects were calculated by averaging the values derived from both sides of the arteries under study. Image noise was defined as the standard deviation (SD) of attenuation within a 2.0 cm^2 ROI in surrounding air on the level of glottis. The axial slice, position and size of the ROIs were kept constant across all reconstructions. CNRs were calculated as: $CNR = (attenution_{vessel} - attenution_{muscle})/noise$.

Subjective image analysis

Subjective analysis was independently performed by two readers with 4 and 3 years of training in neuroradiology. The readers were blinded to all scanning and patient information, and they were allowed to adjust window settings to achieve the best visualisation for each individual patient to achieve the best diagnostic performance. Image quality was subjectively assessed in terms of vessel edge sharpness as well as vascular opacification versus noise. A four-point scoring scale was used: 4 = excellent, with very sharp edges and a high subjective contrast-to-noise ratio; 3 = good, with restrictions due to minimal blurring or slightly suboptimal subjective contrast-to-noise ratio; 2 = moderate but still diagnostic, with considerable restrictions due to the vessel edge blurring or markedly suboptimal subjective contrast-to-noise ratio; 1 = non-diagnostic, with unacceptable blurring or a subjective contrast-to-noise ratio.

Statistical analysis

Statistical analyses were performed with SPSS software (SPSS, version 22.0, Armonk, NY, USA). Quantitative variables were expressed as mean ± SD and categorical variables as frequencies or percentages. $p < 0.05$ was considered statistically significant. Differences in categorical variables (sex ratio and location of injection) were compared using chi-square test. Comparisons between Mixed, Mono and Mono+ images in the LC-CM group were performed by repeated ANOVA analysis with Bonferroni correction. Comparisons between the optimal lowest keV Mono+ images in the LC-CM group and all the series of images in the HC-CM group were performed by one-way ANOVA followed by Dunnett's post-hoc test. The independent sample *t* test for normally distributed data or Mann-Whitney U tests for non-normally distributed data were used to compare the following parameters: differences in patient characteristics (age, weight and body mass index) between two groups, differences in objective image quality parameters (vascular attenuation, noise and CNR) and subjective image quality scores between the optimal lowest keV Mono+ images in the LC-CM group with Mixed images in the HC-CM group. The Shapiro-Wilk test was applied to assess the normality of data distribution. The consistency of the evaluation for image quality by the two radiologists was estimated by kappa test, which was interpreted as poor ($k < 0.40$), moderate ($0.41 \leq k < 0.60$), good ($0.61 \leq k < 0.80$) and very good ($0.81 \leq k < 1.00$).

Results

Scans were successfully completed for each of the 65 patients. There was no significant difference between the HC-CM group and LC-CM group with respect to sex, age, body weight, body mass index or location of injection ($p > 0.05$, Table 1).

Comparison of image quality on monoenergetic (Mono and Mono+) images and Mixed images in the LC-CM group

Assessment of objective parameters among the above images was carried out by evaluating the overall mean CT attenuation and mean CNR for the four arteries.

Mono and Mono+ images showed a consistent increase in vascular attenuations as energies decreased from 100 to 40

Table 1 Patient characteristics

Parameter	HC-CM group (n = 32)	LC-CM group (n = 33)	p
Sex ratio, (male/female)	25/7	21/12	0.199
Age (range), (year)	63.7 ± 9.7 (45-84)	60.7 ± 10.8 (36-81)	0.249
Weight, (kg)	76.0 ± 12.9	70.9 ± 11.1	0.091
Body mass index (BMI; kg/m^2)	26.0 ± 3.6	25.5 ± 3.8	0.596
Location of injection (left/right)	13/19	15/18	0.694

HC-CM: high-concentration contrast medium, LC-CM: low-concentration contrast medium

keV. The largest vascular attenuations were found at 40 keV for the Mono and Mono+ images and no significant differences were observed (Mono: 710.8 ± 88.8 HU; Mono+: 704.3 ± 85.7 HU; p = 0.675) (Fig. 1A, Table 2). Image noise exhibited an increasing tendency from 100 keV to 40 keV in the Mono and Mono+ images. The image noise did not vary greatly between 100 and 60 keV but increased significantly from 60 keV to 40 keV. Image noise at 40 keV with Mono+ was significantly lower compared with Mono (8.6 ± 2.2 HU vs. 15.3 ± 3.7 HU; p < 0.001) (Fig. 1B, Table 2). The CNR in Mono and Mono+ images showed a consistent increasing trend from 100 to 60 keV. From 60 to 40 keV, the CNR decreased in the Mono images and continued to increase in the Mono+ images. Therefore, the CNR of the Mono+ images at 40 keV (78.5 ± 23.5) was significantly superior to that of the Mono images at 40 keV (42.2 ± 10.6) (p < 0.001) (Fig. 1C, Table 2).

Compared with the Mixed images, the 40-keV Mono+ images showed a statistically significant increase of 131% in overall vascular attenuation (704.3 ± 85.7 HU vs. 305.3 ± 41.6 HU; p < 0.001) and a 91% increase in image noise (8.6 ± 2.2 HU vs. 4.5 ± 0.8 HU; p < 0.001). The CNR was increased by 35% (78.5 ± 23.5 vs. 58.0 ± 13.9; p < 0.01) (Fig. 1).

Objective assessment of image quality between monoenergetic (Mono and Mono+) images and Mixed images in the HC-CM group was also performed and the trend was similar to the LC-CM group. Results are shown in the supplementary material (Supplementary Table S1, Fig. S1).

Figure 2 provides a typical image impression of the Mixed and monoenergetic (Mono and Mono+) images investigated in the LC-CM group.

Comparison of image quality on 40-keV Mono+ images in the LC-CM group and all the series of images in the HC-CM group

Assessment of the objective parameters among the above images was carried out by evaluating the overall mean CT attenuation and mean CNR for the four arteries.

The 40-keV Mono+ images in the LC-CM group showed significantly lower vascular attenuations compared with the 40-keV Mono and Mono+ images in the HC-CM group, but significantly higher compared with other series in the HC-CM group (all p < 0.01) (Fig. 3A). Image noise for the 40-keV Mono+ images in the LC-CM group was significantly lower than for the 40-keV Mono images in the HC-CM group (8.6 ± 2.2 vs. 13.5 ± 3.2; p < 0.001) and higher than in others series in the HC-CM group, but there were no statistical differences compared with the 50-keV Mono and 40-keV Mono+ images in the HC-CM group (8.6 ± 2.2 vs.7.9 ± 1.9; 8.6 ± 2.2 vs. 7.3 ± 2.3; both p > 0.05) (Fig. 3B). The CNR for the 40-keV Mono+ images in the LC-CM group was significantly lower than for the 40-keV Mono+ images in the HC-CM group (78.5 ± 23.5 vs. 119.1 ± 52.6; p < 0.05). However, the 40-keV Mono+ images in the LC-CM group showed a comparable CNR with

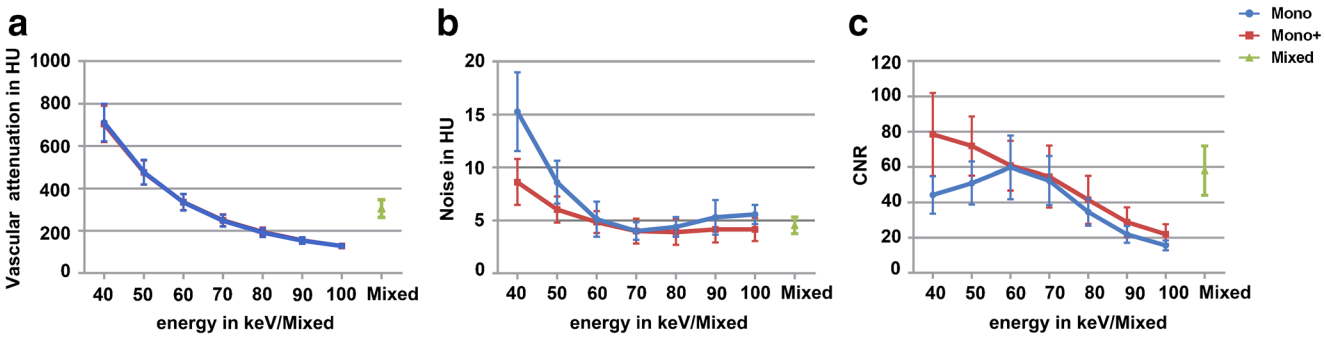

Fig. 1 Curves demonstrate mean vascular attenuation (**A**), image noise (**B**), mean contrast-to-noise ratio (CNR; **C**) of the traditional monoenergetic (Mono, blue line) and advanced monoenergetic (Mono+, red line) images at different energy levels (40 to 100 keV) compared with the standard mixed (Mixed, 120 kVp equivalent) images (green) in the LC-CM group

Table 2 Comparison of mean vascular attenuation, image noise and mean contrast-to-noise ratio (CNR) indices among the standard mixed (Mixed) images, traditional monoenergetic (40, 50, 60, 70, 80, 90, 100) and advanced monoenergetic (40+, 50+, 60+, 70+, 80+, 90+, 100+) images in the LC-CM group at various kiloelectron (keV) levels

	Vascular attenuation (HU)	Noise (HU)	CNR
Mixed	305.3 ± 41.6	4.5 ± 0.8	58.0 ± 13.9
40	710.8 ± 88.8	15.3 ± 3.7	44.2 ± 10.6
40+	704.3 ± 85.7	8.6 ± 2.2	78.5 ± 23.5
50	477.2 ± 57.9	8.6 ± 2.0	51.0 ± 12.2
50+	475.1 ± 56.2	6.0 ± 1.2	72.0 ± 17.0
60	335.1 ± 39.2	5.1 ± 1.7	59.8 ± 18.0
60+	335.6 ± 38.4	4.8 ± 1.0	60.8 ± 14.1
70	247.5 ± 27.7	4.0 ± 0.8	52.3 ± 13.8
70+	249.6 ± 27.4	4.0 ± 1.2	54.6 ± 17.5
80	191.4 ± 20.5	4.4 ± 0.9	34.6 ± 7.8
80+	194.0 ± 20.4	3.9 ± 1.2	41.5 ± 13.6
90	153.9 ± 15.8	5.3 ± 1.6	21.8 ± 4.8
90+	154.7 ± 15.3	4.2 ± 1.2	28.8 ± 8.4
100	128.1 ± 12.8	5.6 ± 0.9	15.6 ± 2.8
100+	128.7 ± 12.1	4.2 ± 1.1	22.0 ± 5.7

HU: Hounsfield unit

most of the images in the HC-CM group including the Mixed images (78.5 ± 23.5 vs. 71.6 ± 20.0; $p > 0.05$) (Fig. 3C).

Comparison of image quality on 40-keV Mono+ images in the LC-CM group and Mixed images in the HC-CM group

The 40-keV Mono+ images in the LC-CM group showed significantly higher vascular attenuations compared with the Mixed images in the HC-CM group on the four levels of the aforementioned arteries, with increases of 126%, 85%, 92% and 82%, respectively (AA: 688.3 ± 100.7 HU vs. 323.7 ± 58.5 HU; CCA: 754.9 ± 91.3 HU vs. 407.0 ± 77.9 HU; ICA: 732.9 ± 104.5 HU vs. 381.8 ± 81.1 HU; MCA: 647.3 ± 92.5 HU vs. 354.8 ± 56.2 HU; all $p < 0.001$) (Table 3). Noise presented a statistically significant 83% rise (8.6 ± 2.2 HU vs. 4.7 ± 1.2 HU; $p < 0.001$) (Table 3). The CNR was slightly higher for the 40-keV Mono+ images in the LC-CM group compared with the Mixed images in the HC-CM group and only on the level of AA showed statistical differences (76.9 ± 21.1 vs. 61.1 ± 16.4; $p < 0.01$) but CCA, ICA and MCA (CCA: 83.7 ± 24.5 vs. 78.1 ± 23.2; ICA: 82.2 ± 26.8 vs. 76.8 ± 24.1; MCA: 72.5 ± 24.6 vs. 70.6 ± 19.2; all $p > 0.05$) (Table 3).

Two radiologists independently assessed the image quality. Scores of observer 1 and observer 2 for the 40-keV Mono+ images in the LC-CM group were 3.94 ± 0.24 and 3.97 ± 0.17, respectively, and for the Mixed images in the HC-CM group, scores were 3.78 ± 0.42 and 3.88 ± 0.34, respectively. There was no statistical difference in subjective image scores between the two groups (3.95 ± 0.19 vs. 3.83 ± 0.35; $p > 0.05$) (Table 4). The inter-observer agreement was good at 40-keV Mono+ images in the LC-CM group (k value = 0.653) and Mixed images in the HC-CM group (k value = 0.676).

Figure 4 provides a general image impression of the Mixed images in the HC-CM group and 40-keV Mono+ images in the LC-CM group.

Discussion

Obtaining high-quality CT images with a low CM dose is a topic of interest in radiology. In single-energy scanning with fixed tube voltage and constant image quality, there is a trade-off between the CM dose and radiation dose because the application of a low CM dose requires a higher tube current, which consequently increases the radiation dose. In our study, however, with the latest Mono+ technique, a reduced CM dose could be used to achieve constant image quality without compromising the radiation dose. Our study investigated the potential to reduce the CM concentration using the Mono+ technique from the cervical and cerebral DE-CTA on a third-generation DS-CT system. It was found that the 40-keV Mono+ images in the LC-CM group showed a comparable objective and subjective image quality compared with the Mixed images in the HC-CM group. Results in this work demonstrated that image quality using LC-CM associated with the Mono+ technique is equivalent to (and even better than) that of the Mixed images in the HC-CM group.

Although beneficial results have been shown for imaging using the traditional Mono technique [13–16], recent studies comparing Mono+ with Mono have demonstrated favourable results for Mono+ because of substantially lower image noise at similar attenuation levels [18–25]. Of them, two studies are pertinent to the evaluation of cervical and cerebral arteries. Schneider et al. [13] showed 60-keV Mono images significantly improved the vascular attenuation and CNR of cervical and cerebral DE-CTA. Riffel et al. [24] found that the Mono+ technique improved the image quality at ultra-low keV in Carotid DE-CTA compared with Mono. The findings of our study confirm prior studies, which demonstrated that the Mono+ technique should be chosen over Mono in cervical and cerebral DE-CTA to improve image quality.

Sigal-Cinqualbre et al. [26] were the first to hypothesise that low-kVp scanning might reduce the iodine load by increasing the vasculature enhancement since the lower effective energy approximates the k edge of iodine. This hypothesis has since been extensively investigated in cervical and cerebral CTA studies by several investigators [27–29]. Recently, the monoenergetic reconstruction technique from DE-CT has been applied to obtain images at low keV levels; it can

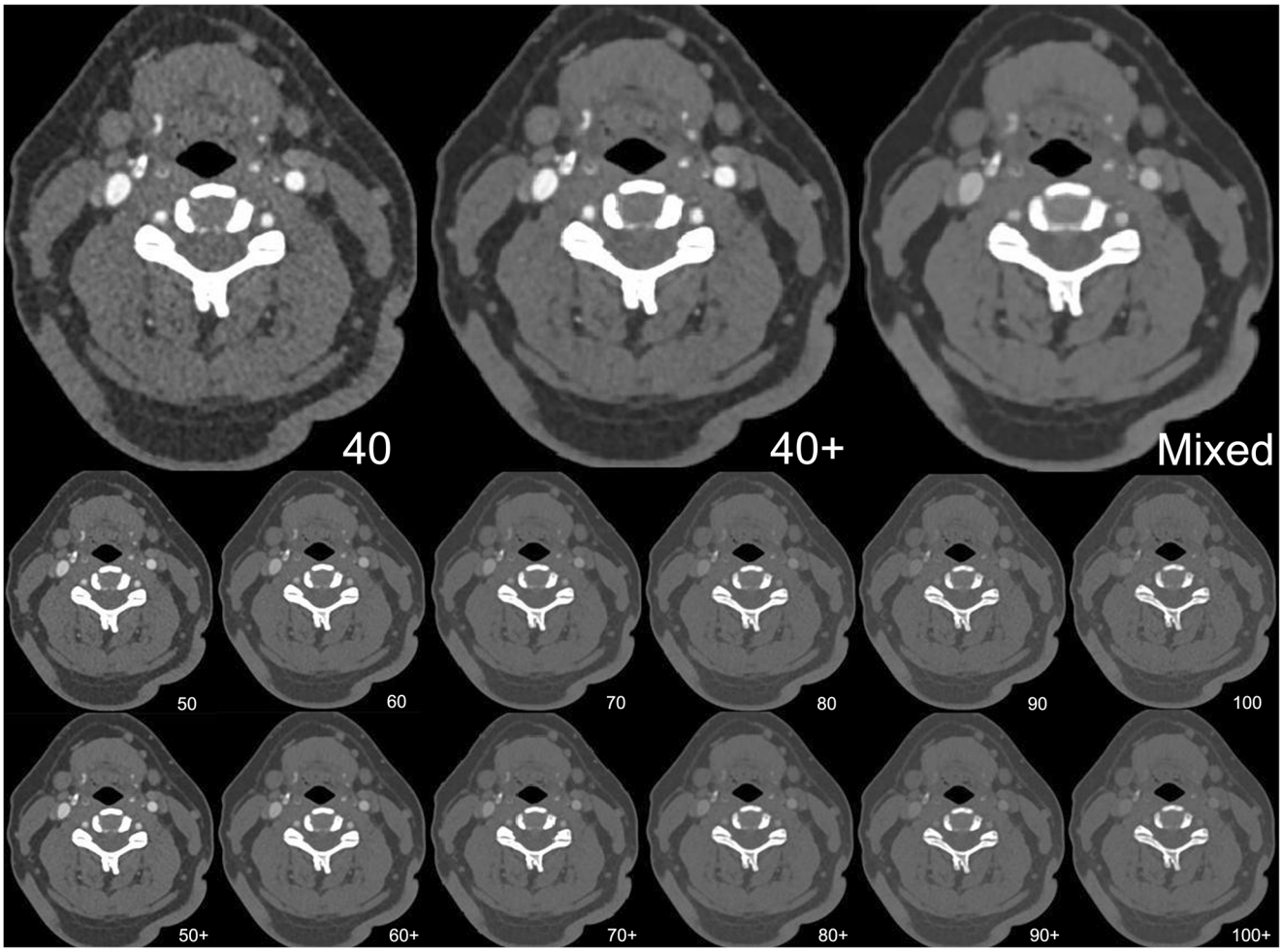

Fig. 2 CT images of a 36-year-old male patient who underwent cerebral and cervical DE-CTA. Images were reconstructed with the traditional Mono reconstruction algorithm (40, 50, 60, 70, 80, 90, 100) and noise-optimised Mono+ reconstruction algorithm (40+, 50+, 60+, 70+, 80+, 90+, 100+) in 10-keV increments. The standard mixed images (Mixed) are shown for comparison. Vascular attenuation was similar between Mono and Mono+ reconstruction algorithms; the Mono+ images show less image noise than the Mono images, resulting in superior CNR compared with the traditional Mono reconstruction algorithm; 40-keV Mono+ images show a higher CNR compared with the Mixed images despite higher noise. Window settings were kept equal for better comparability (width, 1000 HU; level, 150 HU)

produce images of any effective energy levels by calculating two polyenergetic images at high- and low-tube energy. There are some approaches to synthesise monoenergetic images depending on the CT system used to acquire the dual-energy

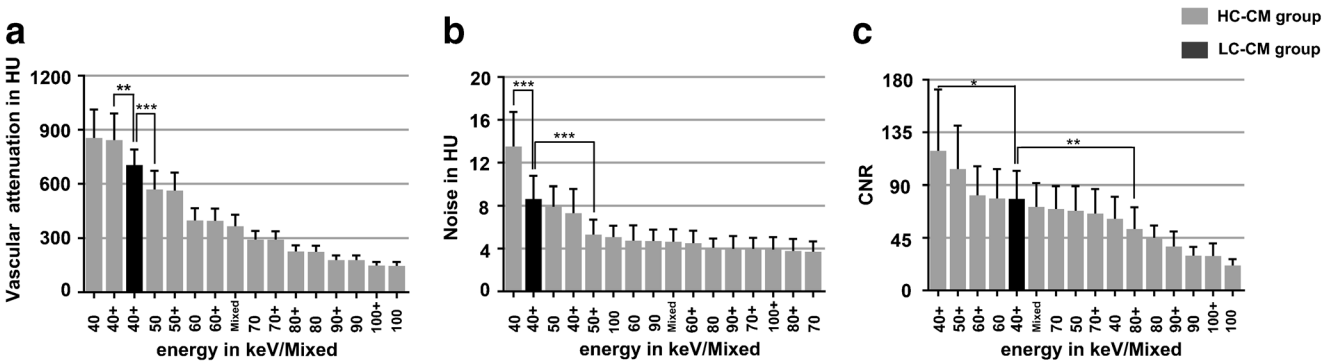

Fig. 3 Mean vascular attenuation (**A**), image noise (**B**), mean contrast-to-noise ratio (CNR; **C**) of the 40-keV Mono+ images in the LC-CM group (black) compared with all the series of images in the HC-CM group (grey). The values are arranged in order from largest to smallest. Statistical differences were marked only in the two reconstructed images with minimum statistical difference in values. (*, ** and *** represent significance where $p < 0.05$, 0.01 and 0.001)

Table 3 Objective image analysis between the standard mixed images in the HC-CM group and 40-keV Mono+ images in the LC-CM group

Group	HC-CM Standard mixed	LC-CM Mono+ 40 keV	Relative difference (%)	*p*
Vascular attenuation (HU)				
AA	323.7 ± 58.8	688.3 ± 100.7	126%	< 0.001
CCA	407.0 ± 77.9	754.9 ± 91.3	85%	< 0.001
ICA	381.8 ± 81.1	732.9 ± 104.5	92%	< 0.001
MCA	354.8 ± 56.2	647.3 ± 92.5	82%	< 0.001
Noise (HU)	4.7 ± 1.2	8.6 ± 2.2	83%	< 0.001
CNR				
AA	61.1 ± 16.4	76.9 ± 21.1	26%	0.004
CCA	78.1 ± 23.2	83.7 ± 24.5	7%	0.555
ICA	76.8 ± 24.1	82.2 ± 26.8	7%	0.967
MCA	70.6 ± 19.2	72.5 ± 24.6	3%	0.52

AA: ascending aorta; CCA: common carotid arteries; CNR: contrast-to-noise ratio; HC-CM: high-concentration contrast medium; HU: Hounsfield unit; ICA: internal carotid arteries; LC-CM: low-concentration contrast medium; MCA: middle cerebral arteries; Mono+: advanced monoenergetic images

data. A few previous studies have evaluated monoenergetic images from a quick switching single-source DE-CT for reducing the iodine load in CTA [30, 31], and some studies evaluated monoenergetic images using the Mono and Mono+ technique from a DS-CTA [32, 33]. Of them, only one study has evaluated the Mono+ technique for reducing the iodine load [33]. In this study, Meier et al. showed that pulmonary DE-CTA with the Mono+ technique is feasible with a reducing iodine load of 6 g and allows for the diagnosis and safe exclusion of central, lobar and segmental pulmonary embolism. To the best of our knowledge, our study is the first to explore the image quality of cerebral and cervical angiography obtained by using the LC-CM and Mono+ technique.

Excellent CNR is an important quality criterion in CTA. By definition, it is derived from both contrast and noise and thus forms the basis for the discrimination of intraluminal contrast material from the surrounding soft tissues, allowing the identification and characterisation of constricted, occluded or poorly opacified vessels [13]. In our study, the 40-keV Mono+ images in the LC-CM group showed comparable image quality in terms of CNR compared with the Mixed images in the HC-CM group. The reason was that the 40-keV Mono+ images could increase the vascular attenuation with less increase in image noise.

Recent studies have shown that appropriate window settings depending on intraluminal HU values are required in monoenergetic images, which differed from the standard settings used in DE-CTA [34–37]. Monoenergetic images at low keV levels increase intravascular attenuations, which require increasing window width for the assessment of calcified plaques. Saba et al. [37, 38] previously described that appropriate window settings could achieve high interobserver agreement in the quantification of the calcified carotid artery stenosis degree. In theory, the attenuation coefficients of calcium and iodine could overlap in low keV levels, making it difficult to distinguish calcification and endoluminal CM.

Importantly, the diagnostic performance of Mono+ images must be considered for cerebral and cervical angiography. Some studies to date have been published on this, but in the evaluation of other vascular structures. Weiss et al. [39] found low keV Mono+ images improve the diagnostic accuracy for the detection of incidental pulmonary embolism in oncological follow-up portal-venous phase dual-energy staging. In other studies, Mono+ images at low keV levels achieved higher CNR values than Mixed images, which led to the improvement of diagnostic accuracy for the detection of endoleaks after endovascular aortic aneurysm repair [40] and active arterial bleeding of the abdomen [41]. In our study, the CNR of

Table 4 Subjective image quality evaluations between the standard mixed images in the HC-CM group and 40-keV Mono+ images in the LC-CM group for two observers

Image	Score	Observer 1				Observer 2			
		1	2	3	4	1	2	3	4
Standard mixed images in the HC-CM group	No.	0	0	7	25	0	0	4	28
40-keV Mono+ images in the LC-CM group	No.	0	0	2	31	0	0	1	32

HC-CM: high-concentration contrast medium; LC-CM: low-concentration contrast medium; Mono+: advanced monoenergetic images; No.: number

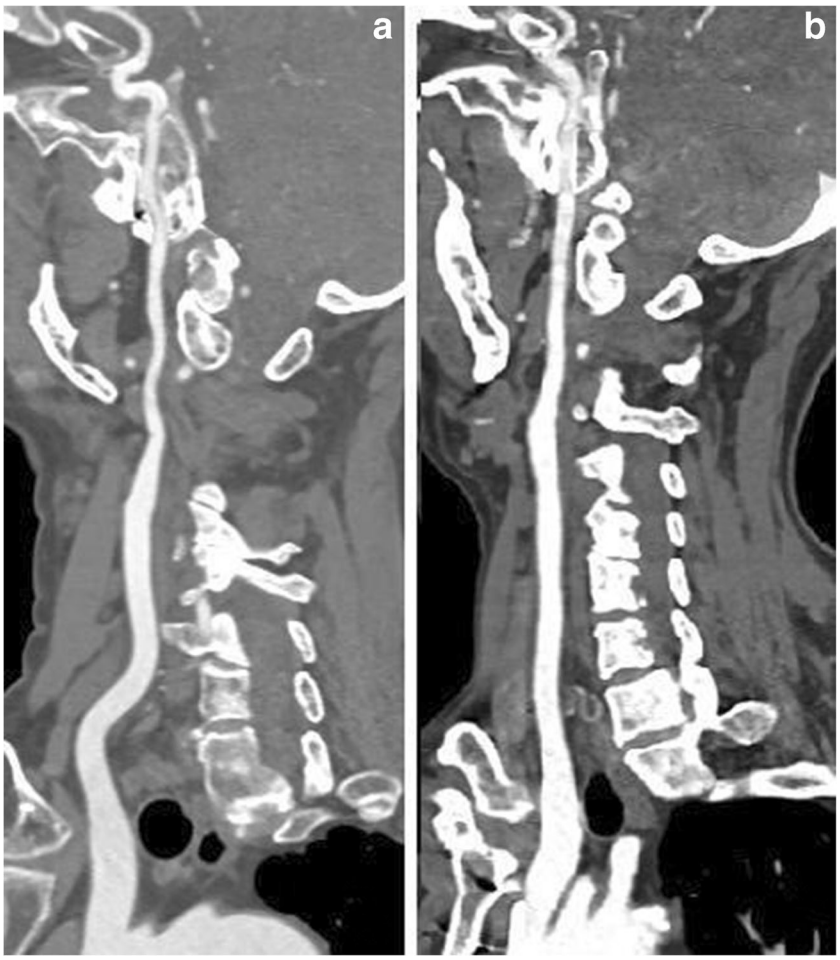

Fig. 4 Examples of image quality of DE-CTA multiple planar reconstruction (MPR) were shown in two patients (**A** and **B**), a 73-year-old female with body weight of 62 kg using 31 ml of 370 mgI/ml contrast medium (**A**) and a 64-year-old female with body weight of 60 kg using 30 ml of 270 mgI/ml contrast medium (**B**); 40-keV Mono+ images in the LC-CM group (**B**) showed higher vascular attenuation and noise compared with the standard mixed images in HC-CM (**A**). Objective and subjective CNR was similar, and both had very sharp vascular edges. Window settings were kept equal for better comparability (width, 1000 HU; level, 150 HU)

40-keV Mono+ images in the LC-CM group was comparable with the Mixed images in the HC-CM group, and therefore the corresponding diagnostic performance in cerebral and cervical CTA could be potentially predicted to be good. This should be assessed in future studies.

In our study, 64 * 0.6-mm collimation for two tubes was used in a 192-slice scanner. Wider collimation allowed a quick scan and a smaller amount of CM; however it would potentially have more cone-beam artefacts. To make small intracranial vessels show well, scanning should not be too fast. So, we used a relatively narrow collimator. Siemens clinically recommends the 80/sn 150-kV tube voltage combination used in this study for cerebral and cervical angiography, so that all images under these two voltages are sufficient for diagnosis while the radiation dose is minimised. It is possible to use the 70/sn 150-kV combination in third-generation DS-CT, which could potentially further reduce the radiation dose. However, the main limitation is that the low-energy photon flux from 70 kV would lead to increased noise, artefacts and reduced vessel visibility in the shoulder regions, especially in obese patients.

This study has some potential limitations. One is the fact that diagnostic performance was not evaluated. Quantitative analysis with variables such as the CNR does not always represent the diagnostic performance; the detection of various plaques, especially calcified plaques, and determination of the stenosis rate, as well as some factors that could influence the diagnostic performance such as beam-hardening artefacts and the window setting should be studied in the two groups in the future. Second, the iodine maps obtained are based on the material separation technique, which may be helpful to distinguish between calcified plaques and endoluminal CM, and it should be investigated in the future. Third, we measured noise in the air, which could lead to paradoxically small SDs because of CT number truncation at -1024 HU in Siemens reconstructions. Extended HU reconstruction or measuring noise in other non-air tissues such as muscles would be preferred. Fourth, the CNR values of the Mixed images in the HC-CM group and 40-keV Mono+ images in the LC-CM group are too high so that there was no subjectively discernible difference between them. Fifth, this study used a low-concentration CM (270 mgI/ml) combined with the Mono+ technique. The results were promising. We could further explore if reducing the total volume of CM while keeping the concentration constant with Mono+ can achieve the same results. Sixth, we only investigated cerebral and cervical arteries combined with the LC-CM and Mono+ technique; we could explore other vessels in future studies.

Conclusions

The image quality of 40-keV Mono+ images with LC-CM was comparable to that of the Mixed (120-kVp equivalent) images with HC-CM. It is therefore concluded that the concentration of iodinated CM might be reduced with the Mono+ reconstruction technique from DS-CT in the diagnosis of cerebral and cervical angiography.

Funding This study has received funding by the Tianjin Research Program of Application Foundation and Advanced Technology (grant 14JCZDJC57000) and National Natural Science Foundation of China (grant 81301217).

Compliance with ethical standards

Guarantor The scientific guarantor of this publication is Dong Li.

Conflict of interest The authors of this manuscript declare relationships with the following companies: Gu Jun is on the speakers' bureau of Siemens Healthineers, Computed Tomography division. The other authors of this manuscript declare no relationships with any companies whose products or services may be related to the subject matter of the article.

Statistics and biometry No complex statistical methods were necessary for this paper.

Informed consent Written informed consent was waived by the Institutional Review Board.

Ethical approval Institutional Review Board approval was obtained.

Methodology
- prospective
- case-control study
- performed at one institution

References

1. Katzberg RW, Barrett BJ (2007) Risk of iodinated contrast material–induced nephropathy with intravenous administration. Radiology 243:622–628
2. Davenport MS, Khalatbari S, Dillman JR, Cohan RH, Caoili EM, Ellis JH (2013) Contrast material-induced nephrotoxicity and intravenous low-osmolality iodinated contrast material. Radiology 267: 94–105
3. Waikar SS, Liu KD, Chertow GM (2008) Diagnosis, epidemiology and outcomes of acute kidney injury. Clin J Am Soc Nephrol 3: 844–861
4. Silver SA, Shah PM, Chertow GM, Harel S, Wald R, Harel Z (2015) Risk prediction models for contrast induced nephropathy: systematic review. BMJ 351
5. Nyman U, Bjork J, Aspelin P, Marenzi G (2008) Contrast medium dose-to-GFR ratio: a measure of systemic exposure to predict contrast-induced nephropathy after percutaneous coronary intervention. Acta Radiol 49:658–667
6. Liu ZZ, Schmerbach K, Lu Y et al (2014) Iodinated contrast media cause direct tubular cell damage, leading to oxidative stress, low nitric oxide, and impairment of tubuloglomerular feedback. Am J Physiol Renal Physiol 306:F864–F872
7. Kitamura O, Uemura K, Kitamura H, Sugimoto H, Akaike A, Ono T (2009) Serofendic acid protects from iodinated contrast medium and high glucose probably against superoxide production in LLC-PK1 cells. Clin Exp Nephrol 13:15–24
8. Bae KT, Heiken JP (2005) Scan and contrast administration principles of MDCT. Eur Radiol 15:E46–E59
9. Cademartiri F, Mollet NR, van der Lugt A et al (2005) Intravenous contrast material administration at helical 16-detector row CT coronary angiography: effect of iodine concentration on vascular attenuation. Radiology 236:661–665
10. Kanematsu M, Goshima S, Miyoshi T et al (2014) Whole-body CT angiography with low tube voltage and low-concentration contrast material to reduce radiation dose and iodine load. AJR Am J Roentgenol 202:W106–W116
11. Zhang C, Yu Y, Zhang Z et al (2015) Imaging quality evaluation of low tube voltage coronary CT angiography using low concentration contrast medium. PloS One 10:e0120539
12. Yu L, Leng S, McCollough CH (2012) Dual-energy CT-based monochromatic imaging. AJR Am J Roentgenol 199:S9–S15
13. Schneider D, Apfaltrer P, Sudarski S et al (2014) Optimization of kiloelectron volt settings in cerebral and cervical dual-energy CT angiography determined with virtual monoenergetic imaging. Acad Radiol 21:431–436
14. Apfaltrer P, Sudarski S, Schneider D et al (2014) Value of monoenergetic low-kV dual energy CT datasets for improved image quality of CT pulmonary angiography. Eur J Radiol 83: 322–328
15. Okayama S, Seno A, Soeda T et al (2012) Optimization of energy level for coronary angiography with dual-energy and dual-source computed tomography. Int J Cardiovasc Imaging 28:901–909
16. Sudarski S, Apfaltrer P, Nance JW Jr et al (2013) Optimization of keV-settings in abdominal and lower extremity dual-source dual-energy CT angiography determined with virtual monoenergetic imaging. Eur J Radiol 82:e574–e581
17. Grant KL, Flohr TG, Krauss B, Sedlmair M, Thomas C, Schmidt B (2014) Assessment of an advanced image-based technique to calculate virtual monoenergetic computed tomographic images from a dual-energy examination to improve contrast-to-noise ratio in examinations using iodinated contrast media. Invest Radiol 49:586–592
18. Meier A, Wurnig M, Desbiolles L, Leschka S, Frauenfelder T, Alkadhi H (2015) Advanced virtual monoenergetic images: improving the contrast of dual-energy CT pulmonary angiography. Clin Radiol 70:1244–1251
19. Albrecht MH, Scholtz JE, Husers K et al (2016) Advanced image-based virtual monoenergetic dual-energy CT angiography of the abdomen: optimization of kiloelectron volt settings to improve image contrast. Eur Radiol 26:1863–1870
20. Martin SS, Albrecht MH, Wichmann JL et al (2017) Value of a noise-optimized virtual monoenergetic reconstruction technique in dual-energy CT for planning of transcatheter aortic valve replacement. Eur Radiol 27:705–714
21. Beeres M, Trommer J, Frellesen C et al (2016) Evaluation of different keV-settings in dual-energy CT angiography of the aorta using advanced image-based virtual monoenergetic imaging. Int J Cardiovasc Imaging 32:137–144
22. Leng S, Yu L, Fletcher JG, McCollough CH (2015) Maximizing iodine contrast-to-noise ratios in abdominal ct imaging through use of energy domain noise reduction and virtual monoenergetic dual-energy CT. Radiology 276:562–570
23. Albrecht MH, Trommer J, Wichmann JL et al (2016) Comprehensive comparison of virtual monoenergetic and linearly blended reconstruction techniques in third-generation dual-source

dual-energy computed tomography angiography of the thorax and abdomen. Invest Radiol 51:582–590
24. Riffel P, Haubenreisser H, Meyer M et al (2016) Carotid dual-energy CT angiography: Evaluation of low keV calculated monoenergetic datasets by means of a frequency-split approach for noise reduction at low keV levels. Eur J Radiol 85:720–725
25. Mangold S, Cannao PM, Schoepf UJ et al (2016) Impact of an advanced image-based monoenergetic reconstruction algorithm on coronary stent visualization using third generation dual-source dual-energy CT: a phantom study. Eur Radiol 26:1871–1878
26. Sigal-Cinqualbre AB, Hennequin R, Abada HT, Chen X, Paul JF (2004) Low-kilovoltage multi-detector row chest CT in adults: feasibility and effect on image quality and iodine dose. Radiology 231: 169–174
27. Zhang WL, Li M, Zhang B et al (2013) CT angiography of the head-and-neck vessels acquired with low tube voltage, low iodine, and iterative image reconstruction: clinical evaluation of radiation dose and image quality. PloS One 8:e81486
28. Kayan M, Demirtas H, Turker Y et al (2016) Carotid and cerebral CT angiography using low volume of iodinated contrast material and low tube voltage. Diagn Interv Imaging 97:1173–1179
29. Luo S, Zhang LJ, Meinel FG et al (2014) Low tube voltage and low contrast material volume cerebral CT angiography. Eur Radiol 24: 1677–1685
30. Almutairi A, Sun Z, Poovathumkadavi A, Assar T (2015) Dual energy CT angiography of peripheral arterial disease: feasibility of using lower contrast medium volume. PloS One 10:e0139275
31. Yuan R, Shuman WP, Earls JP et al (2012) Reduced iodine load at CT pulmonary angiography with dual-energy monochromatic imaging: comparison with standard CT pulmonary angiography–a prospective randomized trial. Radiology 262:290–297
32. Delesalle MA, Pontana F, Duhamel A et al (2013) Spectral optimization of chest CT angiography with reduced iodine load: experience in 80 patients evaluated with dual-source, dual-energy CT. Radiology 267:256–266
33. Meier A, Higashigaito K, Martini K et al (2016) Dual energy CT pulmonary angiography with 6g iodine-A propensity score-matched study. PLoS One 11:e0167214
34. Fu W, Marin D, Ramirez-Giraldo JC et al (2017) Optimizing window settings for improved presentation of virtual monoenergetic images in dual-energy computed tomography. Med Phys
35. De Cecco CN, Caruso D, Schoepf UJ et al (2016) Optimization of window settings for virtual monoenergetic imaging in dual-energy CT of the liver: A multi-reader evaluation of standard monoenergetic and advanced imaged-based monoenergetic datasets. Eur J Radiol 85:695–699
36. Caruso D, Parinella AH, Schoepf UJ et al (2017) Optimization of window settings for standard and advanced virtual monoenergetic imaging in abdominal dual-energy CT angiography. Abdom Radiol (NY) 42:772–780
37. Saba L, Mallarin G (2009) Window settings for the study of calcified carotid plaques with multidetector CT angiography. AJNR Am J Neuroradiol 30:1445–1450
38. Saba L, Mallarini G (2008) MDCTA of carotid plaque degree of stenosis: evaluation of interobserver agreement. AJR Am J Roentgenol 190:W41–W46
39. Weiss J, Notohamiprodjo M, Bongers M et al (2017) Effect of noise-optimized monoenergetic postprocessing on diagnostic accuracy for detecting incidental pulmonary embolism in portal-venous phase dual-energy computed tomography. Invest Radiol 52:142–147
40. Martin SS, Wichmann JL, Weyer H et al (2017) Endoleaks after endovascular aortic aneurysm repair: Improved detection with noise-optimized virtual monoenergetic dual-energy CT. Eur J Radiol 94:125–132
41. Martin SS, Wichmann JL, Scholtz JE et al (2017) Noise-optimized virtual monoenergetic dual-energy CT improves diagnostic accuracy for the detection of active arterial bleeding of the abdomen. J Vasc Interv Radiol 28:1257–1266